SME Digital Manufacturing Challenge 2023
AM to the Rescue: Digital Manufacturing Agility to Address Crises

"On-site Additive Manufacturing of Water Filtration and Decontamination Devices"

Daniel Alves Heinze, Michelle Pomatto, Yiqun Fu.
Advisor: Dr. Christopher B. Williams
Virginia Tech

Executive Summary (5 pt.)

Access to potable water is a critical humanitarian need. It is estimated that 2 billion people worldwide lack access to safe drinking water, and the number is increasing because of climate change and extreme weather events. Thus, an urgent demand arises for an easy-to-use water filtration device that can be made on-site quickly. Herein, we propose the design of a handheld water filtration and decontamination device (WFDD) that can be rapidly fabricated using multi-material fused filament fabrication (FFF) additive manufacturing (AM).

The technical breakthroughs we developed are material with tailored properties and effective geometry design for AM. The geometry of the proposed design is a bottle cap that could be easily screwed onto a plastic bottle. Leveraging the advantages of multi-material FFF printing, the cap consists of a hydrophobic polyethylene terephthalate glycol (PETG) outer case and a hydrophilic perfluorosulfonic acid fluoropolymer (PFSA) filter. PFSA is an ion-containing polymer that can self-assemble its structure through phase separation for use as a membrane. The filter design consists of a thin layer with micron-sized pores and a main core with a field-driven gyroid lattice structure, which can be used to filter fine particles and absorb chemicals. The combination of a macroporous structure controlled by the AM process and a microporous structure controlled by polymer physical chemistry (phase separation) leads to a wide range of membrane separation capabilities.

To validate the proposed design, experimental material characterizations and computational simulations were conducted. First, the materials are proved to be suitable for WFDD. The ability of the materials to block water (outer case) or absorb/permeate water (membrane filter) was verified via characterization of the hydrophobicity of the outer case, hydrophilicity of the filter, water uptake tests, and water permeability. Second, rheological and mechanical measurements were performed to confirm the printability of the selected materials and estimation of printing parameters. Third, a finite element simulation is applied to confirm the structural stability of the cap design is robust. The last, the filtration of the printed core against particles and chemicals was simulated. Our results indicate that the unique design and tailored materials would lead to a reduction in the concentration of chemical contaminants in water by 100 times. Also, the cost of producing the proposed device is calculated as $1.17 per part, lower compared to commercial filter devices. Cost reduction is a bonus to the main goal of this project which is to help save lives by quickly making available water filtration devices.

In conclusion, the development of this project leverages the advantage of AM, such as fast dissemination of design files and on-site manufacturing, as well as the benefits of material design, such as processability and filtration performance. The proposed design was shown to be effective and inexpensive, and its development could largely help aid people in need due to poverty, conflicts, or natural crises.

1. Industry Overview (10 pt.)

According to the latest data from the WHO and UNICEF, 2 billion people lack access to safely managed drinking water at home, and 8 out of 10 people who lack basic drinking water services live in rural areas.[1] These people are in desperate need of reliable access to potable water without relying on manufacturing supply chains that are prone to disruption. Currently, there exist hand-held water purification devices that purify water on demand, such as LifeStraw . However, these systems are manufactured in multiple steps, off-site, and must be shipped worldwide to reach their consumers who are often not in the same country. While this is not a problem for traditional water filtration systems for household use, as the demand is not urgent, it is not effective for emergency situations where a water purification system is needed within days or hours.

There is a huge demand for safe drinking water. According to multiple sources[2-5] including FEMA and the WHO, it is advised to prepare a three-day supply of water prior to a natural disaster occurring, if preparation is possible. FEMA advises one gallon of water per person, per day for a minimum of three days while waiting for emergency relief to provide water or repair damaged water systems. According to a survey from Aquasana,[6] nearly one in three Americans were affected by a natural disaster in 2021 and 77% of those affected reported that it impacted their access to clean drinking water. It is expected that these numbers could be even higher for people in underdeveloped countries or areas of higher populations. In addition, these numbers are expected to increase. According to research,[6] there has been a tenfold increase in the occurrence of global natural disasters since the 1960s with 39 disasters in 1960's to 396 in 2019. That number is projected to increase to 560 by 2030 which averages to 1.5 natural disasters a day. This drastic increase in natural disasters, along with the already established population that lacks clean access to drinking water, establishes the driving factor for the need for quick, cheap access to water filtration devices

To address this need, we propose a comprehensive additive manufacturing solution that integrates the technology's ability to selectively dispense multiple materials, fabricate complex internal structures, and the ability to disseminate digital designs quickly for hyper-local, just-in-time fabrication. Our approach to additive manufacturing handheld water filtration and purification systems enables on-site fabrication of the device when it is needed to provide clean drinking water within hours.

The target consumer would be humanitarian nonprofit organizations such as the WHO, UNICEF, The Red Cross, and Feed the Hungry, as they already have the funding, data, and established connections to the areas that require clean drinking water and would benefit the most from our product. These organizations are also some of the first to arrive in the case of a natural disaster. Our proposed design will meet the needs of quick and cost-effective manufacturing of devices with the capabilities to be manufactured on-site to address the demand for water filtration devices.

2. Design, Functionality and Durability (20 pt.)

The aim of this project is to design a handheld water filtration and decontamination device (WFDD) with multi-materials that can be additively manufactured in a one-step process utilizing a multi-nozzle AM modality. This method of manufacturing will allow the device to be distributed faster to areas in need and require less labor for assembly. The design of WFDD

must be effective and easy to transfer. Therefore, we came up with the design incorporating a bottle cap shape outer case and size grading lattice core filter. The WFDD sketch is shown in **Figure 1**. The WFDD can be simply screwed onto plastic bottles. The core of graded size gyroid lattice design is effective to generate pressure gradient and filtration performance across the WFDD.

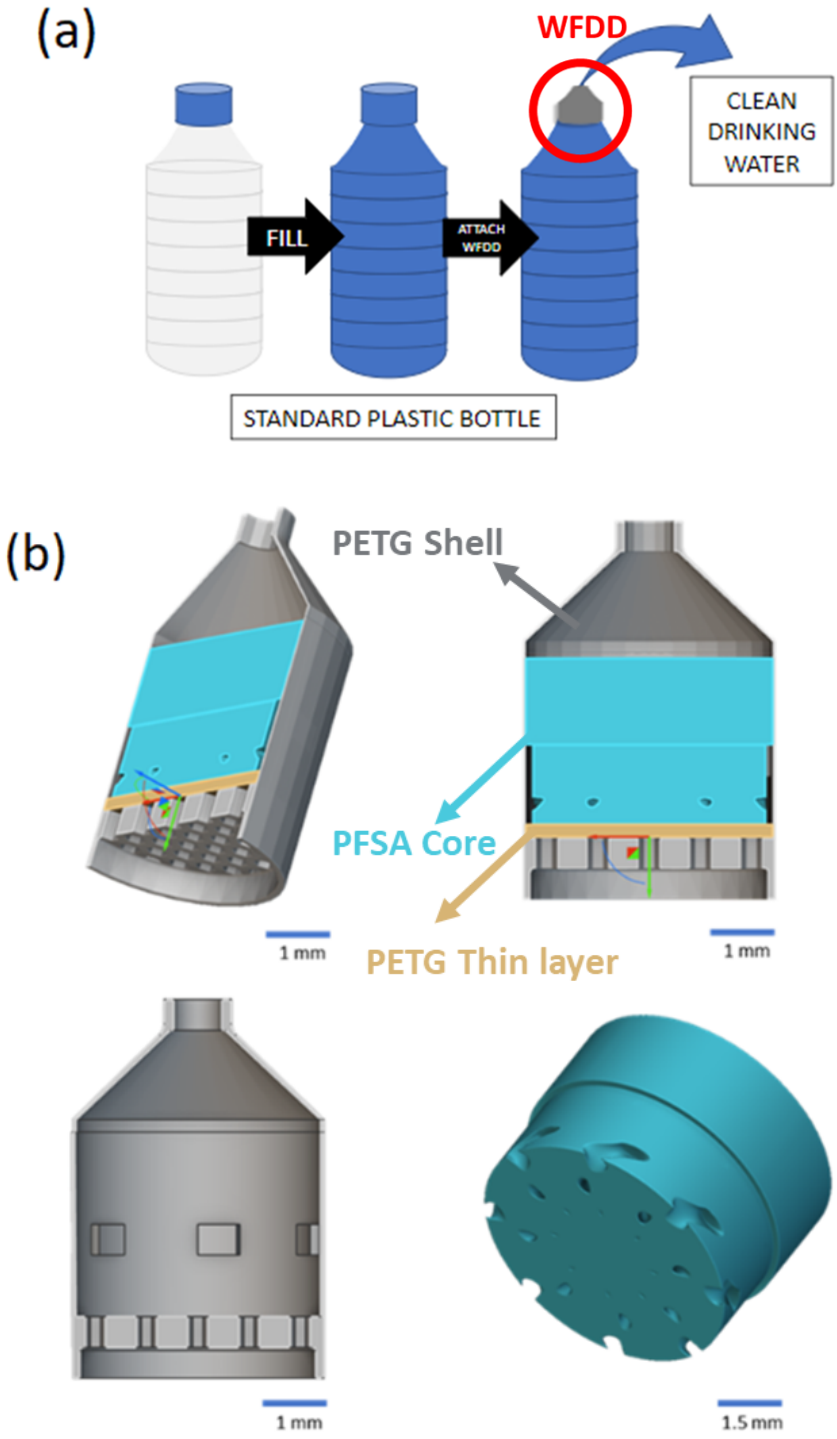

Figure 1. WFDD design sketch. **(a)** The scheme showing the logic of WFDD. **(b)** The geometry of WFDD with cross-section and field-driven designed core (Grey: PETG shell for structure support, orange: thin PETG layer with micron size pores for particle filtration, blue: core made up with PFSA for chemical absorption).

The device is cylindrical, for maximum water flow, and is manufactured from two materials, polyethylene terephthalate glycol (PETG) for shell (outer case) and the thin layer, and a hydrophilic perfluorosulfonic acid fluoropolymer (PFSA) for core. The device can be simply attached to the plastic bottle as a cap (**Figure 1a**). The bottom of the WFDD shell has hexagonal pores with a side length of 0.17 mm to separate relatively large particles. The WFDD shell contains two printed components. The first is a thin PETG layer (0.2 mm) with micron size pores (50 μm) for further particle separation. Next is the main core with a field-driven designed gyroid lattice structure which thickens in the Z direction. The width of the core channel is changing over the thickness of the core. A narrowing channel allows effective particle filtration. This core is utilized to absorb chemicals from the water and very fine particles that pass through the lattice. This hierarchical design largely improves the fluency of the fluid and the efficiency of particles and chemicals filtration.

The shell is made up from PETG, a mechanically strong and hydrophobic material. The PFSA is an ion-containing, mechanically robust, hydrophilic material with systematically designed pore sizes that will be used to print the core with a field-driven lattice. The combination of macroporous lattice designed by geometry and a microporous structure controlled by polymer physical chemistry (phase separation) leads to a wide range of membrane separation capabilities. The membrane processes from microfiltration (pore sizes 50-1000 nm) to nanofiltration (pore size <2 nm) can be controlled through polymer chemistry and polymer physics, and AM design, respectively.

Many polymers and polymer composites have been explored for water purification membranes including poly(vinylidene fluoride) (PVDF), poly(vinyl alcohol) (PVA), polysulfones, glycol-containing polymers, ion-containing polymers, and nanocomposites containing polymer matrix in combination with iron, zirconium, silica, aluminum, clay, carbon and other metal, metal oxide, and/or small inorganic additives.[7] Material selection for this device is critical to meet the goal of the device and compatibility of selected material with the selected AM modality (viscosity, temperature, etc) is acknowledged.

2.1 Product requirements

Product requirements are summarized in Table 1. Firstly, the product must filter 99.999% to 99.999999% of impurities including bacteria, parasites, chlorine, and microplastics. The test methods to determine this include NSF Protocol P231, NSF/ANSI 42, and US EPA guidelines, which are also utilized by other similar products.[8] The product must filter contaminated water fast enough to produce enough water to drink which we have deemed 100 mL/min, a fifth of the flow rate listed by LifeStraw. The product must be low cost and competitive pricing compared to a LifeStraw. The product must be lightweight and reusable for consumers to be able to keep the product on them at all times and be able to produce clean water for drinking at any time necessary. Also, the outer casing must be watertight to prevent loss of filtered water through imperfections in the outer casing, as tested by in-house developed test methods. Finally, the product must meet the engineering requirements of high impact toughness and compressive

strength to withstand everyday use including dropping, stepping on, and/or squeezing the product during use. These requirements may be determined following a test method such as ISO 604. Because this product is to be made on-site, on-demand, the cost per product is not as important as the overall cost of the printer and materials which will be discussed in the process requirements section.

The process requirements are also listed in **Table 1**. Because the WDFF is produced on-site, on-demand, the manufacturing time must be minimized to <1 hr per part. The build volume must be minimum 3 mm x 3mm x 3mm for 1 part. High print accuracy (+/- 0.2 mm) and resolution (≤0.4 mm) is imperative to ensure the field-driven interior gyroidal design dimensions are met as they drive the capture of larger impurities such as dirt from the impure water. The operating costs including material, energy, and labor as well as the base cost of the printer must be minimized to ensure competitive pricing when compared to the purchasing and shipping of other similar products to the desired location. Finally, the print process must be able to simultaneously print multiple materials (outer casing, inner membrane, support) with little to no post-processing and minimal waste production. If post-processing is needed, it must be simple such as physical support removal by hand or by dissolving in water. Due to the remote location of printing, no advanced post-processing techniques would be available.

The last column in **Table 1** lists the material requirements. The materials utilized in the final product must be non-toxic and safe to touch directly after printing (i.e., no monomer, initiator, etc. remaining from the printing process) due to the final use consisting of ingesting water that has passed through the part. In order to be effective, the outer casing must be hydrophobic, to prevent water from exiting through the sides of the part, and the inner material must be made of a hydrophilic material that allows water to pass through it. Due to the wide range of water conditions, both materials must have good pH resistance to withstand both acidic and alkaline water conditions. Additionally, the materials must have high thermal stability (glass transition temperatures above any witnessed temperature) to prevent warpage or melting of the final part. This temperature range was determined to be from freezing point to warm water, 0 C to 50 ^{o}C. Finally, the materials must be printable by the chosen AM modality.

Table 1. Printed WFDD requirements divided into Product, Process, and Material Requirements.

Product Requirements	Process Requirements	Material Requirements
Filters 99.99% of impurities (bacteria, parasites, microplastics) for safe drinking water	Manufacturing Time (<1 hr/part)	Safe - non-toxic materials safe to touch consumables (no monomer, initiator, etc.)
Water flux (>0.25 L/min)	Build Volume (minimum 30 mm x 30 mm x 30 mm)	Hydrophilic (inner membrane sections)
Low cost/ Competitive Pricing (~$20/part)	Print Speed (45 mm/s)	Hydrophobic (outer protective casing)
Lightweight (<100 grams)	High Print Accuracy (+/- 0.2 mm)	Wide pH resistance (basic and acidic water)
Longevity/Reusability (4 L/day for 30 days)	Resolution (≤0.4 mm)	Temperature resistance (0 - 50 ^{o}C)
High Impact Toughness	Operating Costs (materials, energy, labor)	Printable materials (shear thinning if MatEx, correct viscosity, etc.)
High Compressive Strength	Base Cost (machine, training)	High water permeability
Watertight outer casing	Multi-material printing capabilities	
	Little/no post-processing	
	Little/no support material (if needed, must be water soluble)	
	Minimize product waste	

These product, process, and material requirements drive the generation of selection criteria and metrics, as summarized in **Table 2**. The primary goals are to produce a non-toxic product that filters to acceptable levels and can withstand water at different pH levels and temperatures. The product must have acceptable mechanical properties and be produced quickly. Ideally, the associated costs will decrease or be comparable to other similar products on the market once the costs of production, assembly, and shipping have been taken into account.

Table 2. Selection criteria, means of assessment, desired result, and criteria unit.

Selection Criteria	Means of assessment	Desired Result	Units
Non-toxic	Toxicity Tests	Zero	Qualitative
Filtration	Particle Analysis	99.9%	[%]
Water Flux	Water Flow Simulation	Maximize	[mL/min]
pH Resistant	pH Tests	Maximize	[g]
Temperature resistant	Differential Scanning Calorimetry	Maximize	[^{o}C]
Resolution	Machine Quality	Minimize	[µm]
Accuracy	Machine Quality	Minimize	[mm/mm]
Build Volume	Machine Quality	Maximize	[cm]

Print Speed	Machine Quality	Maximize	[cm^3/min]
Operating Cost	Calculation	Minimize	[$]
Base Cost	Calculation	Minimize	[$]
Impact Strength	Simulation	Maximize	[J/m]
Compressive Strength	Simulation	Maximize	[MPa]
Hydrophobic outer casing	Contact Angle	Maximize	[º]
Hydrophilic inner material	Contact Angle	Minimize	[º]
Printable	Rheology - power law index “n”	Shear thinning: n < 1	-

The requirements and selection criteria were then tabulated into a House of Quality chart, shown in **Table 3**. The selection criteria and requirements were related and relative importance was identified using scaling systems rated 9, 3, or 1, with 1 being a weak correlation, 3 being a moderate correlation, and 9 being a strong correlation. The completed house of quality matrix revealed that product lifetime was the most important requirement with material properties of pH resistance, and hydrophobicity being the most important materials criteria, and build volume being the most important process criteria. Accuracy, operating costs and base cost were determined to be the least important.

Table 3. The House of Quality chart.

Improvement Direction:		↑	↑	↓	↑	↓	↓	↑	↑	↓	↓	↑	↑	↑	↓	↓
Legend 9 = strong 3 = moderate 1 = weak	Selection Criteria	Filtration [%]	Water Flux [mL/min]	pH Resistant [g]	Temperature resistant [ºC]	Resolution [mm]	Accuracy [mm/mm]	Build Volume [cm]	Print Speed [cm3/min]	Operating Cost [$]	Base Cost [$]	Impact Strength [J/m]	Compressive Strength [Mpa]	Hydrophobic outer casing [o]	Hydrophilic inner material [o]	Printable [P]
Requirement																
Manufacturing Time						3	1	9	9							9
Product Lifetime		3	3	9	9		1					9	9	9	3	
Low Product Cost				1		1	1	3	1	9	5	9	9			3
Product Leadtime								9	9							3
Minimize Product Waste																9
Watertight		9	9	1	1	3	3					3	1	9	3	1
Effective functionality (filters)		9	9			3	3							3	9	3
Non-toxic (safe for long term use)		9	1	3	1	1	1							1	1	1
Total		30	22	14	11	11	10	21	19	9	5	21	19	22	16	29

The material properties drive the performance of the part and they were ranked highest in importance, as expected. The part will not work properly if the material properties are not correct. The hydrophobicity of the outer casing is vital to ensure the part is mechanically robust and prevents leakage of water from the inside that is being filtered. The hydrophilicity of the

inner material is vital to ensure the material performs the way it is expected to perform and allows water to filter through. However, the costs were the least important, which was surprising, but that may be because the part is very small and the majority of the requirements are materials driven. It is acknowledged that this iteration of House of Quality results may change as the project progresses which may result in other requirements and criteria gaining higher ranking of importance.

2.2 Design simulations

The structural stability of the design is tested through mathematical simulation with corresponding materials properties. Plastic deformation is included to reveal the weak point and if the deformation of the outer case will damage the filter core in the scenario of the part being under a large force. In **Figure 2a** a 500N force is applied at the rim of the bottom shell as the arrows direct. The results show that the stress and most of the deformation are concentrated at the edge. **Figure 2b**. shows the results when 100N force is applied on the lattice surface as arrows direct. It turns out the lattice structure is stable under load holding low stress and little deformation. In short, the design demonstrates the structure stability, proving the design and the materials meet the requirements.

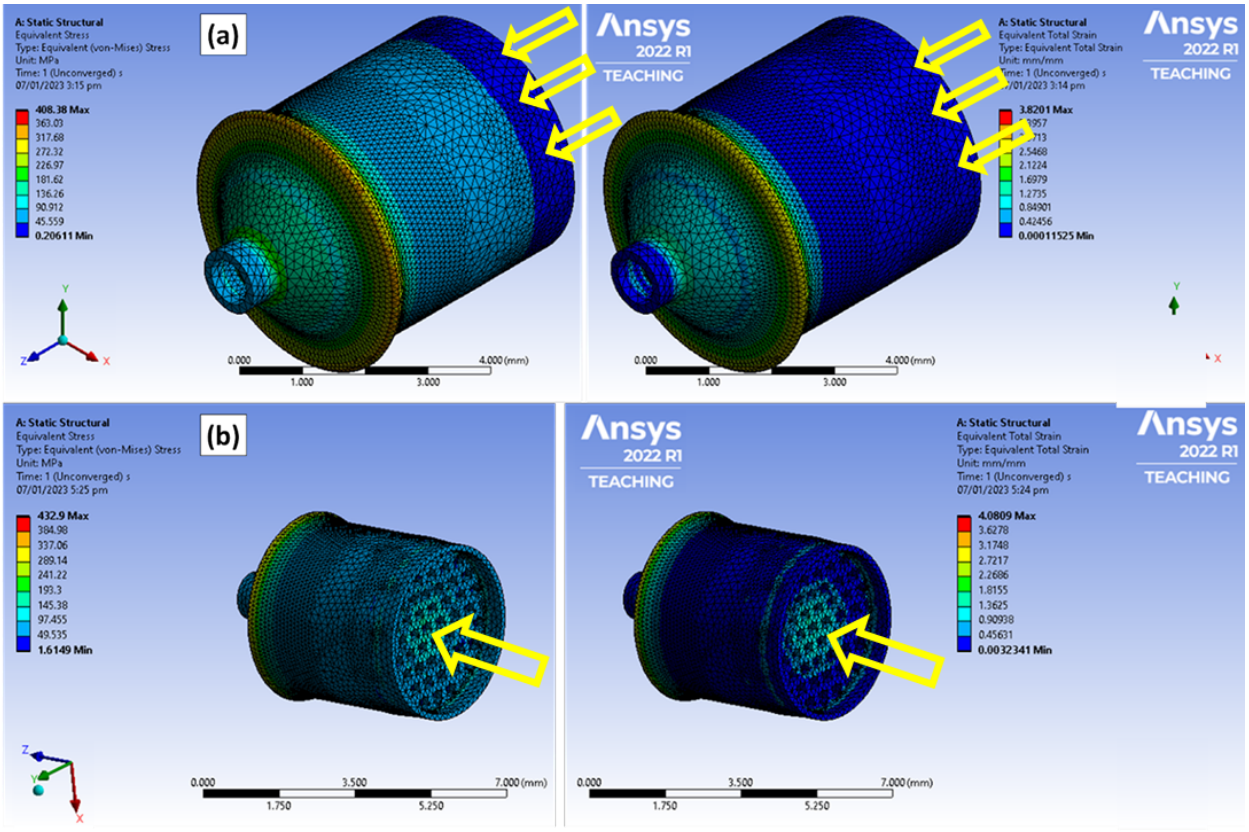

Figure 2. Mechanical simulation of the WFDD shell under load. **(a)** 500N is applied at the rim of the bottom with a fixed support at the nozzle. **(b)** 100N is applied at the lattice of the bottom with a fixed support at the nozzle. All simulations are based on the PET stress-strain curve including plastic deformation.

The filtration performance of the WFDD is also simulated via fluid dynamics and mass transport across porous medium multiphysics. Two types of impurities are considered, particles (e.g. dirt, microplastics, etc.) and chemicals. The material properties of the filter core are listed in **Table 4**. The flow field through the whole part is first simulated by Darcy's Law considering the porous medium characteristics, while the substance transportation and separation are simulated based on the flow field result from Darcy's Law. The results are demonstrated in **Figure 3a**. It shows that the separation of particles is mainly achieved through the first thin layer, which is desired to keep the core from blocking. The core shows an excellent performance on absorption of the chemicals by decreasing the chemical concentration by 100 times. The flow inside the micron channels is simulated with a creep flow model and gyroid channel geometry. The result shows the flow field inside the channels (**Figure 3b**).

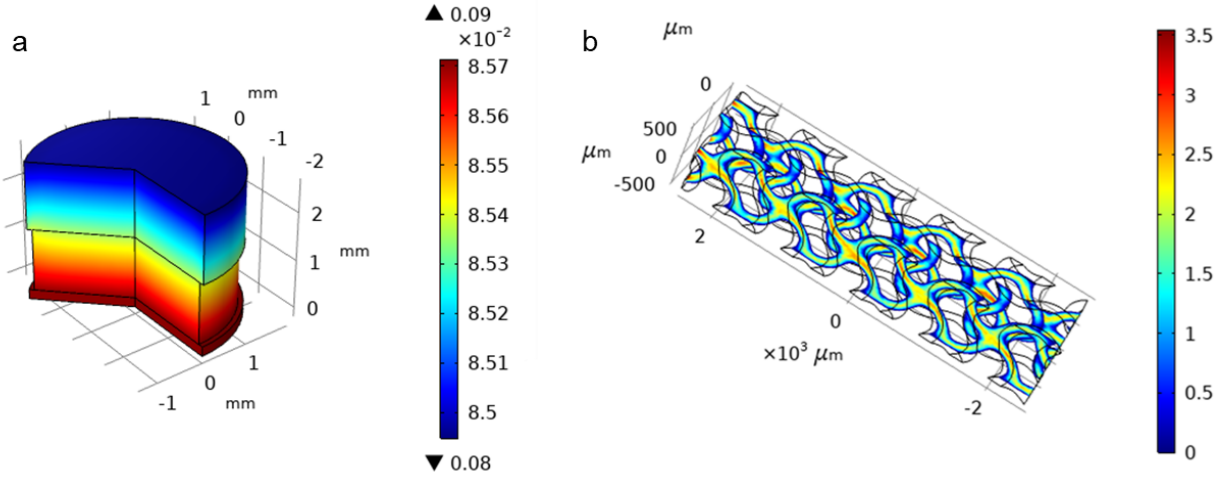

Figure 3. Performance simulation of the WFDD. **(a)** Chemical concentration distribution in the WFDD under steady state. **(b)** Fluid velocity distribution through the micron channels

Table 4. Material properties used in filtration simulation.

Property name	Value used
Porosity of thin layer	20%
Permeability of the thin layer	10^{-11} m²
Porosity of the core	60%
Pore size of the core	50 μm
Inlet pressure	30 kPa
Outlet pressure	0 kPa
Diffusion coefficient of particles	10^{-9} m²/s
Diffusion coefficient of chemicals	10^{-9} m²/s
Freundlich Absorption constant K	10 mol/kg
Freundlich Absorption exponent coefficient N	1

Property name	Value used
Reaction rate	0.4 s^{-1}
Initial chemical concentration	0.085 mol/m^3

3. Design Integration and utilization of DDM materials and processes (20 pt.)

The AM modality best suited for the fabrication of the WFDDs was determined based on the requirements listed in **Table 1** and weighted results from the House of Quality chart in **Table 3**. Multiple AM modalities were ruled out immediately based on the requirements. First, the part will be made with polymeric materials, and so the metal processes like direct energy deposition and metal powder bed fusion are ruled out. Sheet lamination is ruled out due to lack of geometric freedom, the necessity for post processing to finalize material properties, and usage of adhesives that may be water soluble and toxic. The first material requirement of using non-toxic materials meant that no small molecules can be part of the AM process. Vat photopolymerization and material jetting consist of monomer and initiator materials that react to form polymer that provide the resultant part and therefore not viable manufacturing modalities for a WFDD due to the toxic nature of small molecule initiators. Polymer powder bed fusion is a viable option; however, multiple materials are desired in the final product, and PBF is limited to single material prints. Binder jetting of polymeric materials with different types of binder is another option however it would require excessive post-processing and creates large amounts of powder waste and so it is less than desirable. That leaves material extrusion. Material extrusion is possible with non-toxic materials, can consist of multiple print heads to print multiple materials, has the capability to produce water-tight parts when configured correctly, and requires minimal amounts of material per production batch. Material extrusion is also commercially available and widely used in both industrial and personal uses.

Due to the limitations just mentioned, the adaptability of the design for other AM processes would be challenging. For example, the design could be changed to a hollow fiber membrane similar to the LifeStraw filter, where mechanical filtration occurs due to the pore size of the fibers, which would be controlled by the design and printing process. This design could be printed using polymer powder bed fusion with commercially available materials, but removal of powder after printing could be extremely difficult and time consuming. The same concerns are valid for other polymer processes that depend on initiators and monomers that would need to be completely removed after printing to guarantee the safety of the product for human interaction.

Focusing on FFF and thinking about integration with traditional manufacturing, the design could be adapted to a threaded printed filter that screws into a threaded injection molded outside case. This integration could make the production of WDFFs faster, but on the other hand, it would require more assembly and more logistic steps to deliver devices to affected areas, which could actually negatively impact delivery times. As the goal of this project is to have an easy way to print WDFFs on site, the integration of traditional methods could be a setback for the project, and it would largely depend on the capabilities of the affected region with regard to manufacturing infrastructures.

3.1 Material selection

The material selection for this project is a key parameter required for a successful product. Two material requirement analyses were conducted, one for the outer case of the WDFF, and one for the inner part which is responsible for the filtration. With the requirements previously described in mind, PET was chosen for the outer casing because it is a cheap, printable material with a hydrophobic behavior and barrier properties against liquids and gasses. For the filter, two materials were tested to validate the concept, a perfluorosulfonic acid fluoropolymer (PFSA) and a sulfonated polyethylene terephthalate glycol (sPETG) were chosen due to good water uptake, hydrophilicity, and permeability properties. The printability of sPETG is not described in the literature, so material characterization tests were conducted to examine whether this polymer could be made into filaments and printed.

Several sets of experiments were performed to validate the properties and performance of the intended materials and WFDD design. The first material property tested was hydrophobicity of the intended outer casing material, PET, and the intended inner membrane material, PFSA. There are many different types of PFSA with different mechanical and chemical properties but for the sake of simplicity, a commercially available PFSA was utilized for this work. Hydrophobicity is determined by water contact angle using an instrument called a goniometer. A water drop is dropped onto the material and a camera observes the angle at which the water drop is in contact with the material. The smaller the contact angle of water on a material (i.e., the flatter the drop) the more hydrophilic the material. **Figure 4** shows representative images of the water drop angle tests performed on a goniometer with DI water. The contact angle of water on the PFSA membrane, sPETG/PP blend, PETG, and PET were determined to be 20.96, 60.22, 60.88, and 100.05, respectively. It is accepted that a material is considered hydrophobic when its static water contact angle θ is >90° and is hydrophilic when θ is <90°. Therefore, the PFSA is the most hydrophilic, sPETG/PP and PETG are hydrophilic, and PET is hydrophobic, as expected.

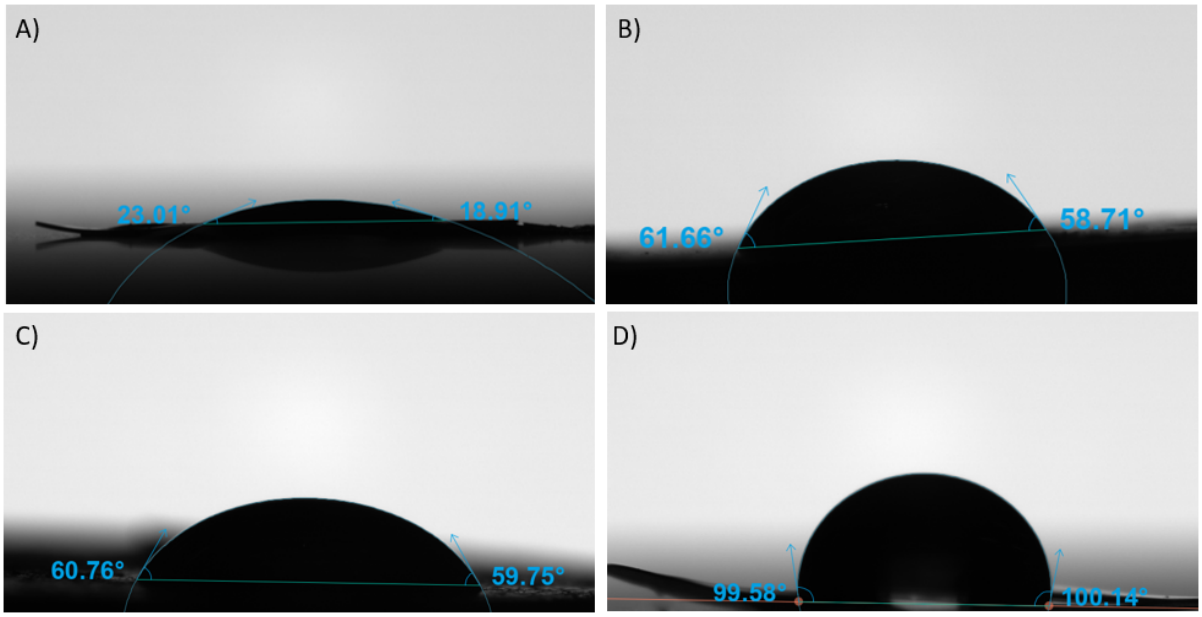

Figure 4. Sensile water drop contact angle images of **(A)** PFSA hydrophilic inner membrane materia;l **(B)** hydrophilic sPETG/PP blended material made into filament and printed; **(C)** printed part from PETG; **(D)** PET film outer casing material. A larger angle indicates hydrophobicity.

The next experiment was a water uptake test. **Figure 5** shows the results from water uptake tests. This test consists of exposing the material to different relative humidities and measuring the increase in weight associated with the adsorption of water. Materials that are hydrophilic will exhibit an increase in weight. Materials that are hydrophobic will not exhibit large increases in weight. A TA QA 5000 TGA-SA under a nitrogen environment was utilized to test the PFSA water uptake. Approximately 10 mg of PFSA was added to the SA platinum sample pan. Weight increase as a function of time was observed by increasing the relative humidity from 0 - 5% and 5% to 95% in increments of 10. **Figure 5** shows that when exposed to humidity over long amounts of time, the inner membrane PFSA material absorbs up to 16% water, confirming this material is hydrophilic. Additionally, the outer casing material, PET, showed no increase in weight, indicative of a hydrophobic material. Establishing that the PFSA material is not only hydrophilic but will uptake water is an important material characteristic and pivotal to the performance of the WFDD.

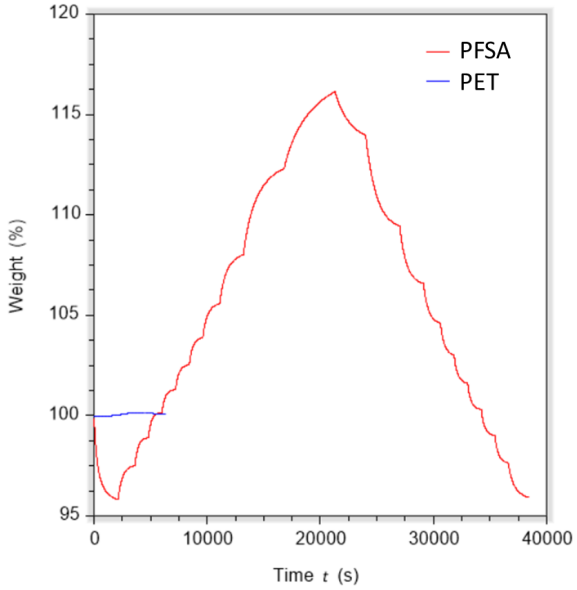

Figure 5. Water uptake measurements of the interior PFSA material (red) and outer casing mastering, PET (blue). PFSA uptakes water with increasing time and humidity

The next experiment was a water permeability test. This test consists of sandwiching a PFSA membrane between two vessels - one that contains orange-dyed water and one that is empty. This test confirms that water will pass through the PFSA material, and due to the microstructure of the PFSA, only very small molecules will pass through. No large particles such as dirt or bacteria will pass through the membrane. **Figure 6** shows the full vessel on the left and the initially empty vessel on the right. After sealing off both sides, a syringe was used to create vacuum in the right vessel which causes water to travel from the left vessel to the right. The progression of water traveling from left to right can be seen as you go from **Figure 6A**, **B**,

C, and **D**. Because the PFSA was previously established to be hydrophilic and uptake water, the results in **Figure 6** are not surprising. This test was only qualitative and a more elaborate test and experimental setup is needed to produce quantitative results on how much water will flow through the membrane over a given time period.

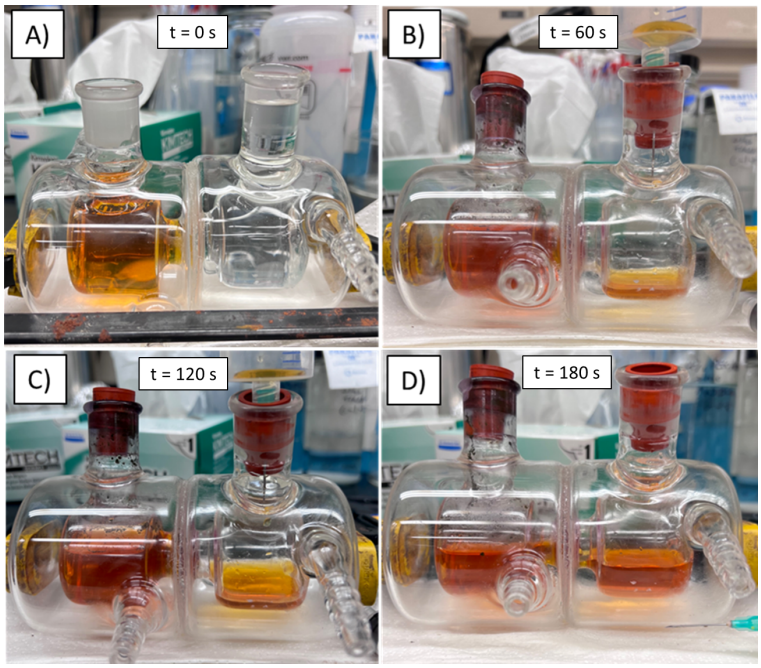

Figure 6. Water permeability experiments with a PFSA membrane sandwiched between two glass vessels containing dyed water (left vessel) and air (right vessel). As a vacuum is created in the right vessel, the liquid passes through the membrane and into the right vessel. The liquid passed through on the scale of seconds, indicated at the top of each image.

3.1.1 Material Printability Results

Steady shear viscosity measurements were performed using a TA Instruments HR-30 torsional rheometer at 235, 250, 265, and 280 °C. A 25-mm parallel plate geometry with a 1 mm gap was used, with the shear rate varying in a logarithmic scale from 0.01 to 6.30 s-1 with 5 points per decade. sPETG/PP disks with 25 mm of diameter and 1 mm of height were made for the tests using a melt press at 250 °C. 20 wt.% PP was added to sPETG to reduce the brittleness of the material. Tests at different temperatures were collected to perform a time-temperature superposition (TTS), expanding the range of shear rates measured to reach printing shear rates between 500 to 10,000 s-1. **Figure 7** shows the time-temperature superposition of the flow sweeps.

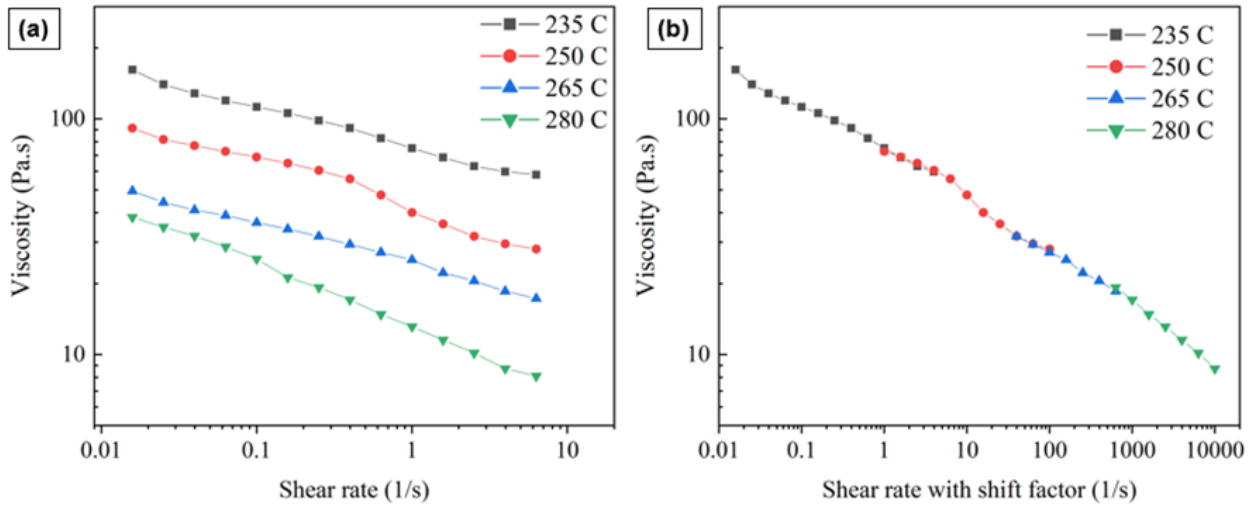

Figure 7. (a) sPETG/PP flow sweeps measured at different temperatures; **(b)** Shifted flow sweep curves at a reference temperature of 235 °C.

The TTS had a good overlap between the curves, expanding the maximum shear rate to 10,000 s-1. The horizontal shift factors used were 15.84, 158.4, and 1584.0 for temperatures of 250, 265, and 280 °C, respectively. These values were chosen empirically to try to maximize the overlap of the curves obtained at different temperatures. No vertical shift factors were needed. **Figure 8** shows a linear relationship between the log of the shift factor and the temperature, further indicating that the TTS applied is valid.

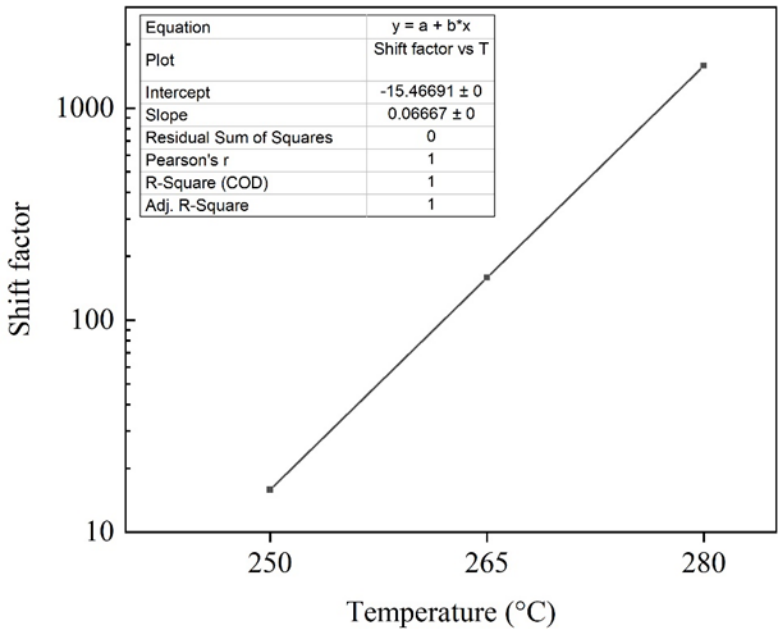

Figure 8. Semilog plot of shift factor vs temperature for sPETG/PP. Fitting indicates a linear relationship of log of shift factor vs temperature.

From the viscosity vs shear rate measurements, a shear thinning behavior is observed, where the viscosity decreased as a function of shear rate. **Figure 9** shows the TTS of viscosity vs shear rate.

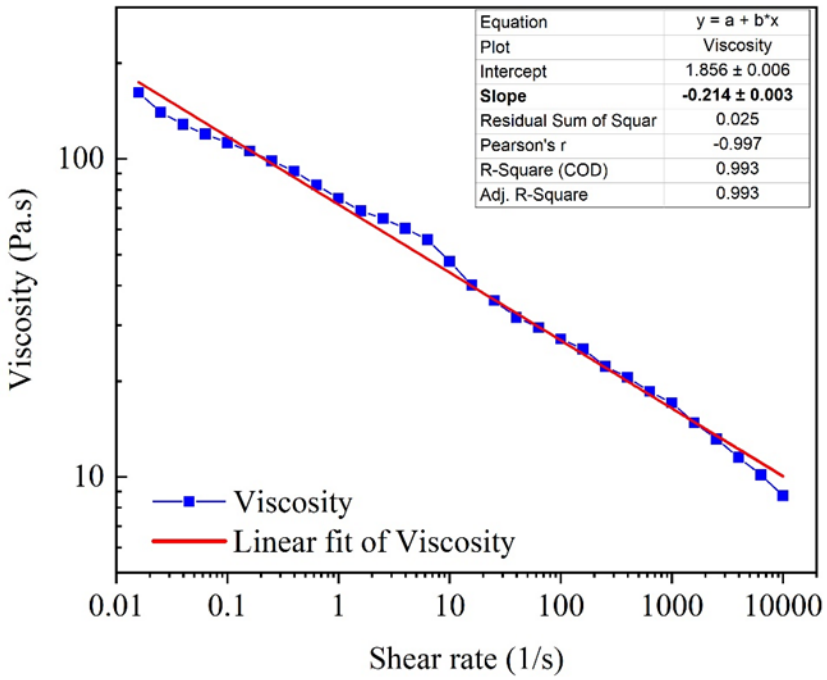

Figure 9. TTS of viscosity versus shear rate at a reference temperature of 235 °C. The linear fitting and fitting parameters of the curves are also shown.

The fitting of this curve yields a slope b of -0.214, which can be used to calculate the power law index n for this material using Equation 1.

$$n = b + 1 \qquad \text{Equation 1}$$

Resulting in a power law index of 0.786. Shear thinning polymers have power law indices smaller than 1, so the value obtained is consistent with what was expected for a shear thinning polymer. Shear thinning is an important requirement for the printability of polymers in FFF, as less pressure is required to extrude the material through the nozzle because the viscosity decreases with increasing shear rates. Equations 2 and 3 describe the volumetric flow during extrusion and the shear rate related to the volumetric flow.

$$Q = r^2 \pi v \qquad \text{Equation 2}$$

$$\gamma = \frac{Q}{\pi r^3}\left(3 + \frac{1}{n}\right) \qquad \text{Equation 3}$$

Where r is the nozzle radius, v is the printing velocity, and n is the power-law index of the polymer. These equations can be combined into a single equation to correlate the shear rates at different printing speeds with different nozzle diameters, as shown in Equation 4.

$$\gamma = \frac{v}{r}\left(3 + \frac{1}{n}\right)$$

Equation 4

Using n = 0.786, calculated shear rates for various printing speeds and nozzle diameters are shown in **Figure 10**.

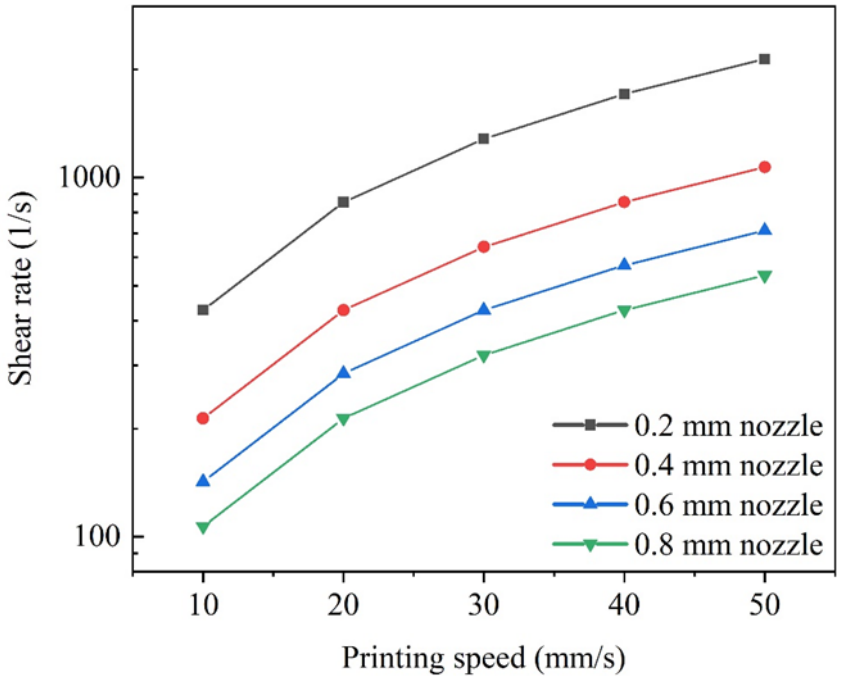

Figure 10. sPETG/PP shear rates calculated for various printing speeds and nozzle diameters.

For the calculated values shown, the smallest shear rate value was approximately 107 s^{-1} for a printing speed of 10 mm/s and a nozzle of 0.8 mm. This shear rate is equivalent to a viscosity of approximately 26.4 Pa.s for the sPETG/PP material. All calculated shear rates are within the range obtained using TTS. With the viscosity data for the whole range of expected shear rates, the pressure required to print can be calculated using Equation 5.

$$\Delta P = \frac{8\eta Q l}{\pi r^3}$$

Equation 5.

Where η is the viscosity, and l is the nozzle length, which is being assumed as 1.6 mm here. **Table 5** lists the pressure values at different printing speeds and nozzle diameters.

Table 5. Pressure drop required to print sPETG/PP at different printing speeds and nozzle diameters.

Printing speed (mm/s)	0.2 mm nozzle	0.4 mm nozzle	0.6 mm nozzle	0.8 mm nozzle
	Pressure drop required to print (kPa)			
10	251.5	72.9	35.3	21.1
20	433.6	125.7	60.9	36.5
30	596.4	172.9	83.8	50.1
40	747.7	216.8	105.1	62.9
50	891	258.4	125.2	74.9

The maximum pressure for the simulated values is 891 kPa for a printing speed of 50 mm/s and a 0.2 mm nozzle diameter. A regular maximum printing pressure was found in the literature as being 570 kPa[9], but other studies have calculated from finite element analysis printing pressures of up to 1640 kPa[10]. Even in the more conservative case, sPETG/PP required pressure should be within the printer limit for all nozzle diameters of 0.4 mm or larger for the printing speeds considered here. The presented results confirm that the sPETG/PP material chosen for the proof of concept can be printed using FFF, as it is shear thinning and its required printing pressure is within printer limit, in accordance with the “printable” metrics defined.

In addition to understanding the viscosity as a function of the shear rate/printing velocity and how that impacts the pressure required from the printer, another source of failure during printing is buckling of the filament before being liquified. Therefore, to measure the resistance of the material to buckling, compression tests were performed on disks of sPETG/PP with a diameter of 25 mm and height of 1 mm. An Instron universal testing machine 5900 series with a load cell of 50 kN was used to collect compressive data of the material at a rate of 2 mm/min. **Figure 11** shows the slope of the compression stress versus the compression strain.

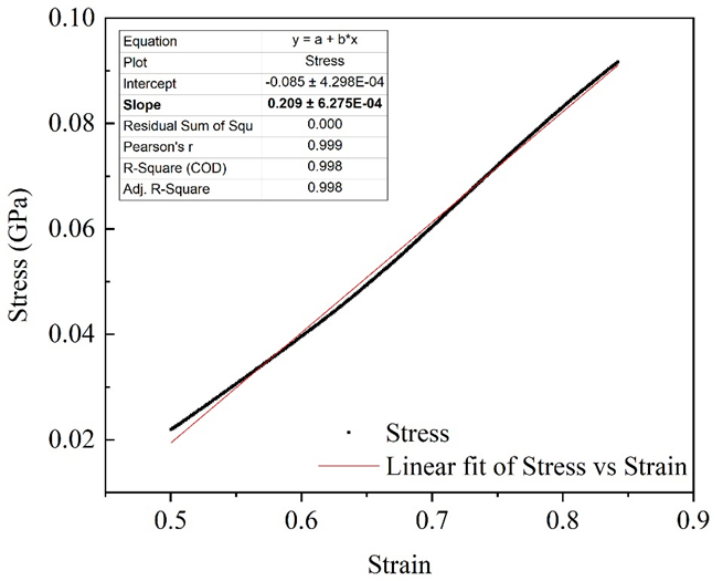

Figure 11. Linear elastic region of the compression test of sPETG/PP disks.

The compression modulus of the material was obtained from the slope of the stress vs. strain curve in the linear elastic region, which is 0.21 GPa. Using the value of the compression modulus, an analysis of the critical region where buckling will not occur can be performed following the procedure by Calafel et al.[11] They argue that for a certain material, buckling will not occur if the relationship shown in Equation 6 follows.

$$\frac{K}{\eta} > \frac{8Ql(\frac{L}{R})^2}{\pi^3 r^4}$$

Equation 6

Where K is the compression modulus, L is the distance between the rollers and the liquefier, and R is the filament diameter. Assuming L as being 60 mm and R as 1.75 mm, we can calculate the left and right-hand sides of Equation 6 to determine whether the filament will buckle. The right-hand side is the critical K/η value, and no buckling should occur if K/η is higher than K/η critical. **Figure 12** shows the curves for four printing nozzle diameters and printing speeds ranging from 10 to 50 mm/s.

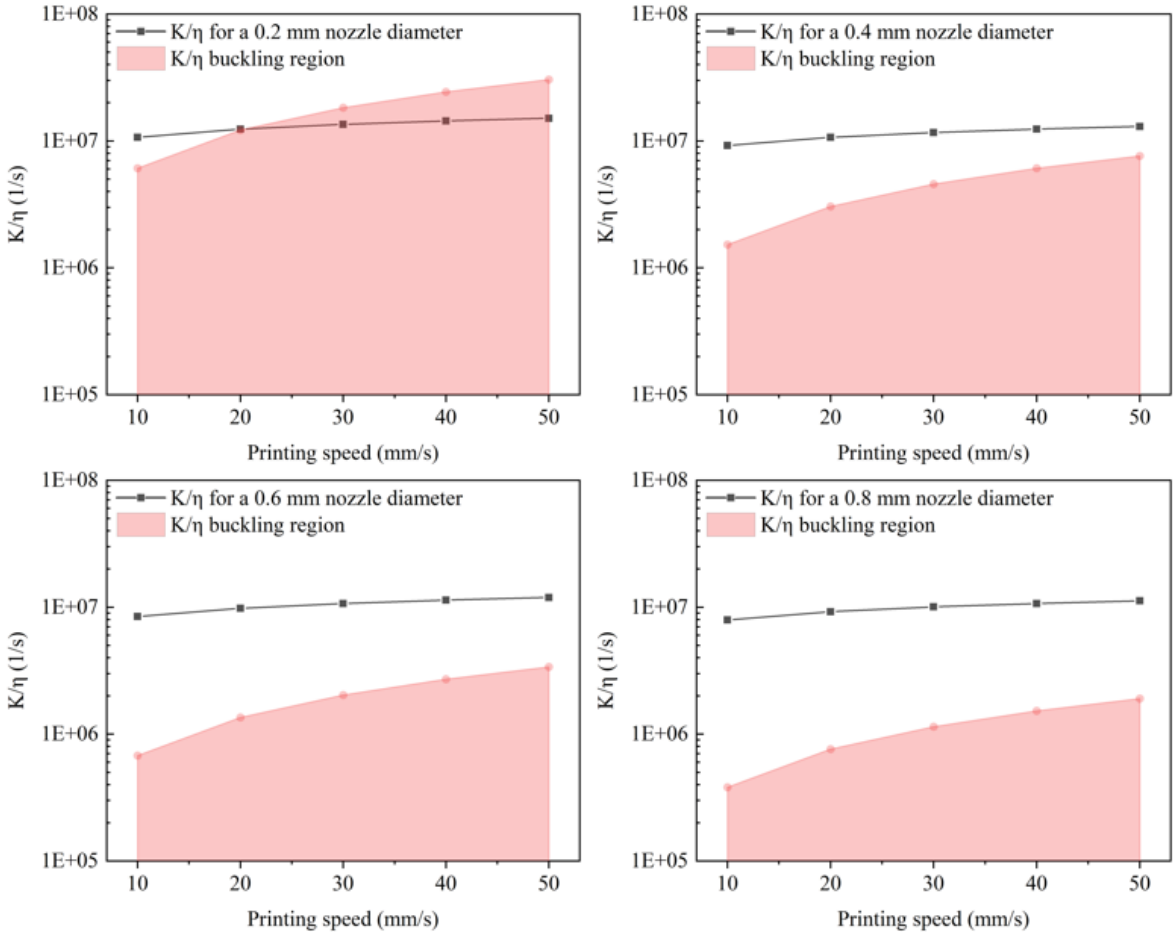

Figure 12. Comparison of buckling parameter vs. critical buckling parameter. No buckling is expected when K/η is greater than K/η critical.

As the printing speed increases or the nozzle diameter decreases, there is an increased likelihood of filament buckling. Buckling would be expected for printing speeds higher than 10 mm/s for a nozzle diameter of 0.2 mm, but for all other scenarios studied here, no buckling would be expected for sPETG/PP filaments.

Material testing indicates that not only the selected materials have the adequate properties to be a suitable filter because they are hydrophilic and have good water uptake and permeability. In addition, its rheological and mechanical properties seem to be in accordance with what is required for a material to be printed in FFF, with a shear thinning behavior of the molten material and good buckling resistance of the filament before melting. As a proof of concept for the structure, a model of the filter was printed using PETG in single material FFF, which is shown in **Figure 13**.

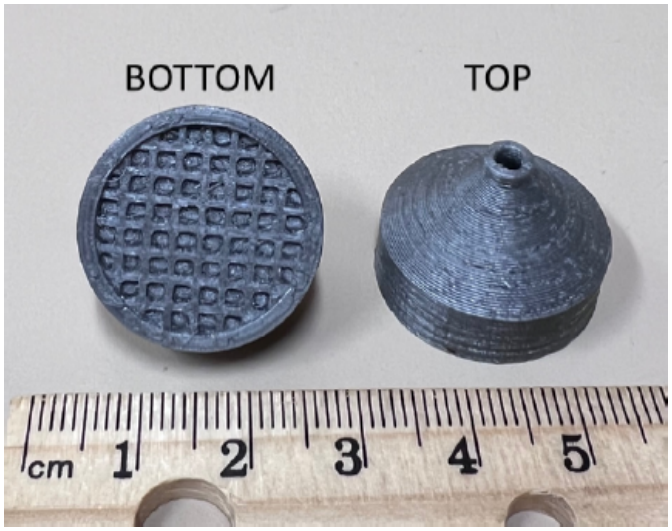

Figure 13. A bottom and top view of a WFDD printed from PETG.

4. Digital and physical infrastructure: Systems integration, utilization, value chain leverage, agility, lean and continuous improvement (20 pt.)

New platforms for the digital dissemination of files would allow for the fast access by affected areas during crises. International humanitarian agencies could have a database of files related to first aid and basic needs for when different crises happen, which can prompt a fast response by instantaneous sharing of information with the affected area.

A successful dissemination and utilization of the printing files would not only depend on digital designs being available for printing, but also on internet, printers, and materials available close to affected areas. An emergency kit with printers/material could be available at different sites around the world by humanitarian agencies to quickly deploy to areas in need. This worldwide digital database of sharable designs to aid in crisis response could eventually even lead to a larger revolution on how AM files are shared, resulting in an easier dissemination/negotiation of other AM designs, which would require new technologies, but specially legislation for the control and sharing of intellectual property.

In addition to extreme cases where crises have happened, WDFF files could be available as a free-of-cost resource for any hobbyist or companies interested in printing them for non-profit use, which could include personal use for traveling, hiking, or for donations to people in need. Clean water availability is one of the United Nations Sustainable Development Goals, and its universal access could be facilitated by the development of an easy to print WDFF.

5. Cost Benefit/Value Analysis (10 pt.)

A cost analysis of the part was performed to determine the economic validity of this design. To perform this step in the design process, it is important to consider every possible cost that could accumulate. Costs can originate from many areas. Not only does the team need to consider the cost of the materials and the machine, but the costs of labor to run the machine as well. Another thing that could impact the cost is whether it is fixed or variable. As more units of the product are produced, the cost of material will increase. An accurate cost analysis will help to ensure the overall success of the product. To calculate the cost per part of an additively manufactured product, the following formula can be used. P represents the purchase price of the machine, O represents the machine operation cost, M represents the material cost, and L represents the labor cost. N is the number of parts in a build. Based on the build plate size (300 mm x 400 mm for CreatBot DE Plus), and the size of the WFDD, it was determined that N=45 parts could be printed per batch. Combining all of these factors gives an accurate estimate of the total cost that it takes to produce one part. Each of these variables are broken down into other contributing factors and individually calculated. **Figure 14** shows the final calculated price per build based on the machine purchase price.

$$\text{Cost per part} = \frac{(P + O + M + L)}{N} = \$1.17$$

$$P = \frac{PurchasePrice * T_b}{0.95 * 24 * 365 * 5\ years} = \$1.80/build$$

$$PurchasePrice = \$5{,}000$$

$$O = T_b * C_o = \$25.65\ per\ build$$

$$T_b = T_{extrude} + T_{transition} = 15\ hrs$$

$$T_{extrude} = 900\ mins \quad T_{transition} = 10\ mins$$

$$C_o = \$1.71/\text{hr}$$

$$C_o = \$15{,}000\ per\ year\ and\ 8{,}760\ working\ hours$$

$$M = k_s * v * C_m * \rho * N = \$10.84\ per\ build$$

$$M = 1.3 * \left(\frac{\$60.75}{kg} * \left(\frac{0.004kg}{part} * 0.75\right) + \frac{\$1.04}{kg} * \left(\frac{0.004kg}{part} * 0.25\right)\right) * 45$$

$$L = T_l * C_l = \$14.42\ per\ build$$

$$C_l = \$28.84/hr$$

$$T_l = 0.5\ hr/part$$

$$N = 45$$

Figure 14. Calculations for the cost analysis of the filter.

P was calculated based on the purchase price of the machine, the time it takes to build a part (Tb), and the number of hours that the machine will be running, likely for a duration of five

years. The build time was calculated by loading the part into Ultimaker Cura and slicing it for an estimate of how long it would take to finish the print. This time was then multiplied by the number of parts that will be printed in one cycle. The time to transition to the next print was also included in the total build time, which was assumed to be 10 minutes. This is enough time for an employee to remove the parts from the build plate and prepare the machine to run again. For the purchased 3D printer, the CreatBot DE Plus was chosen. It has triple extrusion nozzles that will be required for printing both the hydrophobic outer shell and the inner lattice filter design. The triple nozzles will also enable the supports to be printed from a separate, water soluble material. This will make it easy to post-process the filters once they are printed, and will not require any additional equipment or chemical treatments. This printer also has a heated build volume, which will allow better layer adhesion to improve the quality of the printed parts. The build plate is also large enough to print parts in batches, which will increase the overall output of the printer.

In order to find O, the machine operating cost, both the time to build (Tb) and operating cost per hour (Co) were used. The yearly operating cost of the machine was estimated to be about $15,000 per year. The machine will ideally be running nonstop the entire year to maximize profits, which means it will be under operation for 8,760 hours. This is the most expensive part of the production because a high volume of parts will be printed in each batch. However, printing in large batches has proven to lower the cost drastically and will ensure the product stays profitable. The cost of labor per hour was calculated based on paying an employee a salary of $60,000 per year, and a 40 hour workweek for the entire year. Lastly, the material cost M was calculated to be used in the formula for the overall cost of producing a part. M was found using the support material found in the part (ks), the volume of the part (v), the material cost per kilogram (Cm), and the density of the part (p). The mass of the part was found to be 0.0482 kg using the STL file in Fusion 360. Because the part is made up of two different materials, PFSA and PET, the material cost was estimated based on the amount of PFSA and PET utilized in the final part. It is estimated that 75% of the part will be PFSA and 25% PET. The costs of the FSA, PET, and PETG materials are $60.75/kg, $1.04/kg, and $50/kg, respectively. Using these values, the cost of material per part printed was calculated.

The overall cost per part was determined to be $1.17 after using the calculated values in the final formula shown in **Figure 14**. The costliest areas of the design are labor costs and machine operating costs. To keep these costs down, it is important that the machine is kept operating for as many hours as possible throughout the year. If the machine is not running, profits are being lost. It is also possible that labor costs could be reduced from this initial estimate. Once the machine has started printing, no labor is required until the print is finished. Optimizing this process to print for the most possible time while requiring the least oversight from employees will lead to a lower product cost. This product's main competitor in the industry is the Lifestraw, which sells for $20. This design proves to be much cheaper than the Lifestraw because of its compact nature and the ability to print it in large batches. By purchasing an industrial three nozzle FFF printer with a large build volume the product can be built in the most efficient way possible.

Even though a cost reduction may be observed from the proposed design compared to commercial products available, it is important to note that the main goal of this project is not only to reduce the price of the product, but to have a large social, health, and safety impact on

communities affected by crisis or with a lack of access to safe water due to poverty, lack of infrastructure, or conflicts. Creating new routes for the treatment of water that can be easily deployed, locally produced, and rapidly distributed could largely improve the average life expectancy of communities and their quality of life, leading to a return of investment that cannot be estimated with money. Investment in technologies for the well being of humans worldwide should be a top priority in an era where science and technology advances at such fast paces.

6. Conclusions (10 pt.)

The goal of this project was to develop a water filtration and desalination device that could be printed solely by additive manufacturing utilizing material extrusion. A small bottle-cap-sized filtration design was chosen to increase the number of printable parts per print bed and print speed. This design also was lightweight and simple to use with existing bottles. It is acknowledged that other designs could work better- such as a long tube/straw design that more closely resembles the Lifestraw. However, for this project, only one iteration of the design was explored due to time limitations and the number of prototype print limitations. A set of product, process, and material requirements were identified and used to guide the design, material, and process selection. After identifying the key metrics as being the filtration and water flux performance of the material, its safety (pH and temperature resistant, resolution and accuracy of the part), delivery time and costs, mechanical strength, hydrophobicity (outer casing) and hydrophilicity (filter), and printability, and comparing them using a house of quality chart, it was determined that material extrusion was the best additive manufacturing modality due to its rapid build time, ability to process non-toxic materials, multiple material capabilities, and relatively cheap cost compared to other AM modalities. The multiple materials chosen and tested for material properties were PETG which is a water soluble support material, PET for the outer casing material, PFSA as a sulfonated hydrophilic material for the inner membrane, and a sulfonated PETG blended with PP to demonstrate sulfonated materials are printable with material extrusion.

A test part was printed utilizing PETG. This test part was printed with PETG in two different orientations and the best orientation was decided to be with the wide base of the part being printed first. Printing in other orientations caused rough surfaces after the removal of support material which was undesirable. The final printed part was printed accurately, but more detailed measurements are needed to accurately measure the inner gyroidal structure of the part to compare to the CAD model.

Material properties of hydrophobicity, water uptake, and permeability were tested and the properties of the materials matched the desired properties. Finite element simulations were performed which verified the structural stability of the part and the ability for water to flow through the part. A field-driven gyroidal design which thickened in the Z direction was utilized to filter out impurities while allowing water to flow through.

A cost analysis showed that the price per part would be $1.17, $18.83 less than the lead competitor, Lifestraw, due to its compact design which allows for multiple parts to be printed on the build plate. A summary of the testing results compared to the identified criteria in **Table 2** is shown in **Table 6**. Due to the time and testing instrument limitations, toxicity, filtration and pH resistance were not explored. The chosen materials of PET, PFSA, and PETG passed the criteria for material properties. The economics of the print are promising due to the small size

and minimal material and print time, as discussed previously. The mechanical properties that were simulated showed positive results indicating that the design is mechanically robust to withstand intended use.

Table 6. Selection criteria and results from testing, simulations, and calculations. A pass or fail is indicated in the Results column.

Selection Criteria	Means of assessment	Desired Result	Units	Results
Non-toxic	Toxicity Tests	Zero	Qualitative	PASS (according to literature)
Filtration	Particle Analysis	99.90%	[%]	Could not test
Water Flux	Water Flow Simulation	Maximize	[mL/min]	PASS
pH Resistant	pH Tests	Maximize	[g]	PASS (according to literature)
Temperature resistant	Differential Scanning Calorimetry	Maximize	[°C]	PASS
Resolution	Machine Quality	Minimize	[µm]	PASS
Accuracy	Machine Quality	Minimize	[mm/mm]	PASS
Build Volume	Machine Quality	Maximize	[cm]	PASS
Print Speed	Machine Quality	Maximize	[cm3/min]	PASS
Operating Cost	Calculation	Minimize	[$]	PASS
Base Cost	Calculation	Minimize	[$]	PASS
Impact Strength	Simulation	Maximize	[J/m]	PASS
Compressive Strength	Simulation	Maximize	[MPa]	PASS
Hydrophobic outer casing	Contact Angle	Maximize	[°]	PASS
Hydrophilic inner material	Contact Angle	Minimize	[°]	PASS
Printable	Rheology - power law index “n”	Shear thinning: n < 1	-	PASS

References

[1] Access to Clean Water, Sanitation, and Hygiene. Centers for Disease Control and Prevention. https://www.cdc.gov/healthywater/global/wash_statistics.html#:~:text=2%20billion%20people%20lack%20access,have%20basic%20drinking%20water%20service. Access 12-14-2022.

[2] Food and Water in an Emergency. Federal Emergency Management Agency (FEMA). https://www.fema.gov/pdf/library/f&web.pdf. Access 01-08-2023.

[3] Water Sanitation and Health: Humanitarian emergencies. World Health Organization. https://www.who.int/teams/environment-climate-change-and-health/water-sanitation-and-health/environmental-health-in-emergencies/humanitarian-emergencies. Access 01-08-2023

[4] Emergency Water. Loma Linda University. https://home.llu.edu/campus-spiritual-life/emergency/emergency-water. Access 01-08-2023

[5] PREPARING AND STORING AN EMERGENCY SAFE DRINKING WATER SUPPLY. University of Florida. https://edis.ifas.ufl.edu/publication/SS439. Access 01-08-2023

[6] Survey Reveals Concern About Natural Disasters & Clean Water Access. Aquasana. https://www.aquasana.com/info/natural-disasters-affect-drinking-water-survey-pd.html. Access 01-08-2023

[7] Bassyouni, M., Abdel-Aziz, M. H., Zoromba, M. S., Abdel-Hamid, S. M. S., & Drioli, E. (2019). **A review of polymeric nanocomposite membranes for water purification**. Journal of Industrial and Engineering Chemistry, 73, 19–46. doi:10.1016/j.jiec.2019.01.045

[8] LifeStraw Go: Product Guide. LifeStraw. https://help.lifeStraw.com/article/131-lifestraw-go. Access 01-08-2023

[9] Duty, C., Ajinjeru, C., Kishore, V., Compton, B., Hmeidat, N., Chen, X., … Kunc, V. **What makes a material printable? A viscoelastic model for extrusion-based 3D printing of polymers**. Journal of Manufacturing Processes, 35, 526–537. (2018) doi:10.1016/j.jmapro.2018.08.008

[10] Ramanath, H.S., Chua, C.K., Leong, K.F. et al. **Melt flow behaviour of poly-ε-caprolactone in fused deposition modelling**. J Mater Sci: Mater Med 19, 2541–2550 (2008). https://doi.org/10.1007/s10856-007-3203-6

[11] Calafel, I., Aguirresarobe, R. H., Peñas, M. I., Santamaria, A., Tierno, M., Conde, J. I., & Pascual, B. **Searching for Rheological Conditions for FFF 3D Printing with PVC Based Flexible Compounds**. Materials, 13(1), 178. (2020) doi:10.3390/ma13010178